On the Normal Component of Centralized Frictionless Collision Sequences

Pieter J. Mosterman
The MathWorks, Inc.
3 Apple Hill Dr.
Natick, MA 01760
USA

December 15, 2003

Abstract

A typical assumption for rigid body collisions with multiple impact points is that all collisions occur simultaneously and are synchronized in their compression/expansion behavior, a useful assumption given the microscopic time-scale at which collisions occur. In case collisions are dependent upon one another, however, there is interaction between and within compression and expansion phases. Instead of treating the collisions as separate consecutive impacts or by activating all constraints at the same time, a rule is presented that orders the collisions as a sequence of *interacting* events at a point in time to handle the normal component of the collisions.

Keywords: hybrid modeling, systematic model abstractions, parameter abstraction, time scale abstraction, collision behavior.

1 Introduction

This paper discusses a collision rule for the normal component of sequences of frictionless collisions based on the canonical case of centralized impact. Collision behavior of rigid bodies is an extensively studied problem in the field of mechanics, see, e.g., (Brach 1991; Chatterjee & Ruina 1998; Glocker 1995; Ivanov 1995; Pfeiffer & Glocker 1996), and the overview (Brogliato 1999), and can be divided into studies on single and multiple collisions. In case of multiple collisions, the underlying assumption is that there are several contact points in the mechanical systems that exhibit collision behavior at the same point in time. Moreover, the decomposition

of the collision effect into a compression and expansion phase is assumed to be synchronized, i.e., all collisions are simultaneously first in their compression and next in their expansion phase.

This assumption has proven accurate for collisions that are initiated by evaluating macroscopic dynamic behavior. However, if collisions become dependent such that one collision triggers another, the separate collision phases do not occur simultaneously even though in a macroscopic view still at the same point in time.

For example, consider the three colliding bodies in Fig. 1. It is assumed there is centralized frictionless impact, so only the behavior along the normal component needs to be evaluated. There are two contact points, one between m_1 and m_2, contact 12, and one between m_2 and m_3, contact 23. If upon collision of m_1 with m_2 the collision between m_2 and m_3 is evaluated simultaneously, for certain restitution coefficients (ϵ) results may be generated that contradict a first order linearized (spring-damper) approximation (Mosterman & Breedveld 1999).

To make this intuitive, consider the bodies have equal mass, m, and collisions are perfectly elastic, i.e., $\epsilon^{12} = \epsilon^{23} = 1$. At the time of collision, m_2 and m_3 are at rest, so, there is no restitution of relative velocity. Therefore, if executed simultaneously, the collision between m_1 and m_2 appears to be between a body with mass m and a body with mass $2m$, and, consequently, m_1 will obtain a velocity with opposite sign. However, from experiments it is known that m_1 should (almost) come to rest, a result that is derived from evaluating the collisions in sequence. Because of the dependency between the collisions, for $\epsilon^{12} = \epsilon^{23} = 1$ it is critical to evaluate the collisions in sequence.

For other restitution coefficients quite the opposite is true. Consider again a perfectly elastic collision between m_1 and m_2 ($\epsilon^{12} = 1$), but combined with a perfectly non-elastic collision between m_2 and m_3 ($\epsilon_{23} = 0$). In this case, a linear first-order approximation of the collision behavior between m_1 and m_2 *does* approximate that of a collision between one body with mass m and another with mass $2m$, and m_1 obtains a velocity with opposite sign. However, if the idealized collisions are evaluated in sequence, first m_1 transfers its momentum to m_2, and next this is distributed over m_2 and m_3 to obtain equal velocities of half the initial magnitude.

These observations are discussed in detail in previous work (Brogliato 1999; Mosterman & Breedveld 1999) which explicates the necessity for either a pairwise evaluation or simultaneous evaluation, depending on the coefficientes of restitution. This is a rather unsatisfying phenomenon, especially since it leaves unclear for which ϵ to switch between the different evaluations. This paper seeks to overcome this by introducing a pre-collision stage preceding dependent collisions, computed based on Newton's collision rule. This presents a rule for modeling sequences of dependent collisions that converges uniformly between the limit

values.

2 Collisions Reviewed

On a macroscopic scale, collision behavior can be modeled by (i) the equations of motion that describe relative velocities and acceleration and forces at the contact points and (ii) the contact conditions, i.e., the conditions that determine whether the collision equations of motion are active. In addition, it is required to find contact points, i.e., perform collision detection, which is beyond the scope of this paper.

The distance between two bodies at a contact point, i, is given by g_N^i, the relative velocities at a contact point by $\dot{g}_N^i$ and the constraint force in the normal direction by λ_N^i. Methods for computing these values immediately before collision are described in detail elsewhere, e.g., in (Glocker 1995; Pfeiffer & Glocker 1996). In the following, because of the assumptions that the collision is without friction, at center, and only occurs in the normal direction, the subscript N can be removed, as all variable values are given in the normal direction.

2.1 A Linear Approximation

To evaluate the accuracy of the collision rules, at least in a gross sense, a linear first-order spring-damper (RC) collision approximation for the system in Fig. 1 is used as a reference. The velocity values after the collision are presented in Table 1 for several parameter combinations (simulations are performed with the hybrid bond graph simulator HyBrSim (Mosterman & Biswas 1999; Mosterman 2002)). Here, the damper parameters R^{12} and R^{23} capture the dissipation of the collision between m_1 and m_2, and m_2 and m_3, respectively. Similarly, the linear approximation of the elasticity is captured by C^{12} and C^{23}. The initial state is $v_1 = 1$, $v_2 = 0$, and $v_3 = 0$, where $v_j,\ j \in \{1, 2, 3\}$, is the velocity of mass m_j.

Two mass distributions are evaluated; one where $m_1 = m_2 = m_3 = 1$ and the other where $m_1 = m_2 = 1$ and $m_3 = 1000$. The latter corresponds to an example in other work (Pfeiffer & Glocker 1996) where a ball is bounced off another ball that is at rest on a floor, see Fig. 2. The dissipation is varied between large and small values to serve as a reference for $\epsilon \approx 0$ and $\epsilon \approx 1$, respectively, in the idealized case. Note that the linear model is a rough approximation of the real collision phenomena, and only valid as a rather qualitative indication.

2.2 Collision Rules

The equations of motion can be described by a Newton or Poisson type collision rule. Newton's rule specifies the collision at a contact point in terms of the relative velocity before, $\dot{g}_A$, and

after the collision, $\dot{g}_E$,[1]

$$\dot{g}_E = -\epsilon \dot{g}_A \tag{1}$$

where ϵ ($0 \leq \epsilon \leq 1$) is the *coefficient of restitution* that determines the energy that is dissipated during the collision. For $\epsilon = 0$, the collision is *perfectly nonelastic* and there is maximum dissipation, for $\epsilon = 1$, the collision is *perfectly elastic* and there is no dissipation.

Poisson's collision rule is formulated on the force level and consists of a compression and expansion stage. During the compression stage, a force builds up till the relative velocity between the colliding bodies has vanished, the velocities of the individual bodies at this point are indexed by C, e.g., v_C. This force is then applied during the expansion stage. In the idealized collision model, these compression and expansion phases occur instantaneously at the same point in time, but ordered so that the expansion phase begins immediately after the compression phase is completed. So, the compression and expansion forces become impulsive, Λ_C and Λ_E, respectively. To account for dissipation, the return impulse is modified by a coefficient ϵ

$$\Lambda_E = \epsilon \Lambda_C \tag{2}$$

Note that computationally this coefficient ϵ is not the same as the coefficient of restitution, ϵ, used in Newton's collision rule. However, conceptually they are similar in that they capture the degree of elasticity of the collision. Therefore, and in order not to produce excessive, and to an extent superfluous, notation, the same variable ϵ is used in the proceedings.

Given the equations of motion, the contact conditions still need to be specified to completely capture collision behavior. In case of the unilateral constraints of collision phenomena, the complementarity formulation can be used. This formulation states that (i) when the bodies are touching, $g^i = 0$, there can be a positive force between them, $\lambda^i > 0$, and (ii) when the bodies are disconnected, $g^i > 0$, there is no force between them, $\lambda^i = 0$. This can be formulated in a compact set of constraints

$$g^i \geq 0;\ \lambda^i \geq 0;\ g^i \lambda^i = 0 \quad \forall i \in I^G \tag{3}$$

where I^G is the set of all possible contact points. Typically (Glocker 1995; Lötstedt 1981; Pfeiffer & Glocker 1996), these complementarity constraints are formulated on the acceleration level, in which case the g^i variable is replaced by $\ddot{g}^i$

$$\ddot{g}^i \geq 0;\ \lambda^i \geq 0;\ \ddot{g}^i \lambda^i = 0 \quad \forall i \in I^G \tag{4}$$

The use of the complementarity principle in physical system modeling is discussed in more detail elsewhere (Chatterjee 1999). Other work (Mosterman & Breedveld 1999) has used

[1] Notation is derived from (Glocker 1995). Contact points will be superscripted whereas reference to bodies around contact points and their variables are subscripted.

a state transition formulation to determine whether contact exists and whether a collision occurs.

In (Glocker 1995), the collision conditions for applying Newton's collision rule are

$$I^N = \{i \in I^G | g^i = 0; \dot{g}^i \leq 0\} \tag{5}$$

So, the relative distance has vanished and the relative velocity is towards each other. The condition for applying Poisson's collision rule, though, is

$$I^P = \{i \in I^G | g^i = 0\} \tag{6}$$

The reason for this is that to ensure the bodies do not penetrate in case of multiple contacts, Newton's collision rule requires stricter assumptions. Because Poisson's collision rule breaks down in two phases, it can be evaluated whether penetration will occur given the compression impulses in an intermediate evaluation and at this point it can be corrected by allowing arbitrarily large impulses. Note that this implies that the collisions are evaluated simultaneously.

2.3 Example

In accordance with Table 1, the differences in behavior are illustrated by two mass distributions, $m_1 = m_2 = m_3 = 1$ and $m_1 = m_2 = 1,\ m_3 = 1000$, for the system in Fig. 1 with varying degrees of elasticity for the respective collisions.

2.3.1 Newton

For the system in Fig. 1, upon vanishing of g^{12}, it is evaluated whether $\dot{g}^{12} \leq 0$, which is true. Also, $g^{23} = 0$ and $\dot{g}^{23} \leq 0$, so the collision rule generates

$$(v_{2,E} - v_{1,E}) = -\epsilon^{12}(v_{2,A} - v_{1,A}) \tag{7}$$

$$(v_{3,E} - v_{2,E}) = -\epsilon^{23}(v_{3,A} - v_{2,A}) \tag{8}$$

In addition, the forces have to be balanced, i.e., $F_1 + F_2 + F_3 = 0$, which has the instantaneous equivalent (conservation of momentum)

$$m_1(v_{1,E} - v_{1,A}) + m_2(v_{2,E} - v_{2,A}) + m_3(v_{3,E} - v_{3,A}) = 0 \tag{9}$$

This combines into a set of three equations with three unknowns, and it can be solved for $v_{j,E},\ j \in \{1, 2, 3\}$.

Figure 3 shows the velocities computed from evaluating these constraints for varying ϵ^{12} and ϵ^{23} and fixed $\epsilon^{23} = 1$ and $\epsilon^{12} = 1$, respectively. Note that, because $(v_{3,A} - v_{2,A}) = 0$,

$v_{3,E} = v_{2,E}$. For $m_1 = m_2 = m_3 = m$ and $\epsilon^{12} = 1$, the results equal a collision between a body with mass m and one with mass $2m$, which represents anomalous behavior because momentum should be completely transferred from m_1 to m_3.

In case m_3 becomes very large, Fig. 3(b), it remains almost at rest and because $(v_{3,A} - v_{2,A}) = 0$ the same holds for m_2. In terms of Fig. 2, using Newton's collision rule, m_2 never leaves the floor, which contradicts the results for a linear approximation in Table 1. This is conform the analysis in (Pfeiffer & Glocker 1996) and circumvented by Poisson's collision rule.

2.3.2 Poisson

For the Poisson collision rule, upon vanishing of g^i, first the impulsive forces because of the compression phase are computed. This results in ($v_{i,C}$ are the velocities at the end of the compression phase)

$$\Lambda_C^{12} = -m_1(v_{1,C} - v_{1,A}) \tag{10}$$

$$\Lambda_C^{23} = m_3(v_{3,C} - v_{3,A}) \tag{11}$$

where the minus sign is determined by the chosen reference point and present because the forces between the bodies work in the opposite direction. This introduces two additional variables which requires two more equations that come from the constraint that at the end of the compression phase the relative velocity is 0, so

$$v_{1,C} = v_{2,C} \tag{12}$$

$$v_{2,C} = v_{3,C} \tag{13}$$

With the equations

$$\Lambda_E^{12} = \epsilon^{12}\Lambda_C^{12} \tag{14}$$

$$\Lambda_E^{23} = \epsilon^{23}\Lambda_C^{23} \tag{15}$$

and conservation of momentum

$$m_1(v_{1,C} - v_{1,A}) + m_2(v_{2,C} - v_{2,A}) + m_3(v_{3,C} - v_{3,A}) = 0, \tag{16}$$

it can be solved for $v_{1,C}$, $v_{2,C}$, $v_{3,C}$, Λ_C^{12}, Λ_C^{23}, Λ_E^{12}, and Λ_E^{23}. Instead of Eq. (14) and Eq (15), the following complementarity problems are solved

$$(\Lambda_E^i - \epsilon^i\Lambda_C^i)\dot{g}_E^i = 0 \tag{17}$$

to ensure either Poisson's rule is applied (the left factor) or the relative velocity vanishes (the right factor). So, the impulse Λ_E^i is computed by Poisson's collision rule, or by ensuring there is no penetration.

In the example in Fig. 1, for equal masses and $\epsilon^{23} = 1$, the following sequence of values is obtained for $\epsilon^{12} < 0.25$

$$\begin{bmatrix} v_1 \\ v_2 \\ v_3 \\ \Lambda_1 \\ \Lambda_2 \end{bmatrix} = \begin{bmatrix} v_0 \\ 0 \\ 0 \\ 0 \\ 0 \end{bmatrix}, \begin{bmatrix} \frac{1}{3}v_0 \\ \frac{1}{3}v_0 \\ \frac{1}{3}v_0 \\ \frac{2}{3}v_0 \\ \frac{1}{3}v_0 \end{bmatrix}, \left(\begin{bmatrix} \frac{1}{3}(1-2\epsilon^{12})v_0 \\ \frac{2}{3}\epsilon^{12}v_0 \\ \frac{2}{3}v_0 \\ \frac{2}{3}\epsilon^{12}v_0 \\ \frac{1}{3}v_0 \end{bmatrix} \right), \begin{bmatrix} \frac{1}{6}v_0 \\ \frac{1}{6}v_0 \\ \frac{2}{3}v_0 \\ \frac{1}{6}v_0 \\ \frac{1}{3}v_0 \end{bmatrix} \tag{18}$$

where the vector in parentheses contains the values that would have been obtained if instead of the complementarity constraints in Eq. (17) to prevent penetration of m_1 and m_2, Eq. (14) and Eq (15) were used. To prevent penetration, an arbitrarily large impulse is computed from the $\dot{g}^{12} = 0$ constraint, in this case, $\Lambda_E^{12} = \frac{1}{6}v_0$. If $\epsilon^{12} \geq 0.25$ there is no penetration and the vector values in parentheses give the final collision values.

Figure 4 shows the resulting velocities for varying ϵ^{12} and ϵ^{23}. Clearly, in case $\epsilon^{23} = 1$, the collision rule does not return values conform the linear approximation in Table 1. Also, for fixed $\epsilon^{12} = 1$, behavior in Fig. 4(c) shows no dependence on ϵ^{23}, although this is expected from the linear approximation (compare the $\{R^{12}, R^{23}\}$ entry $\{0.05, 0.05\}$ in Table 1 with entry $\{0.05, 50\}$).

For a large mass m_3, approximating the setup in Fig. 2, this collision rule does predict m_2 leaving the floor, in accordance with the linear first-order approximation in Table 1 (entry $R^{12} = 50$ and $R^{23} = 0.05$), but for the other limit case $\epsilon^{12} = 1$ and $\epsilon^{23} = 1$, its prediction deviates from the linear first-order approximation (entry $R^{12} = 0.05$ and $R^{23} = 0.05$).

3 A Uniformly Converging Formula

As illustrated in Section 2, the collision effects based on Newton and Poisson rules do not provide satisfactory results for centralized frictionless dependent collision sequences for all coefficients of restitution, $0 \leq \epsilon^i \leq 1$. To design a formula that does, the behavior of a first order linear approximation of the collision sequence in Fig. 1 is first analyzed, see also (Mosterman & Breedveld 1999). For two different damper parameters of the collision between m_2 and m_3 ($R^{23} = 0.05$ and $R^{23} = 5$) the collision behavior is shown in Fig. 5. From this it can be seen that the larger the dissipation between m_2 and m_3, i.e., the less elastic the collision, the less the difference in relative velocity that is allowed.

This observation leads to the conjecture that the velocity of bodies in contact, not immediately partaking in a collision, follow each other closer or not, depending on the elasticity between them. The velocity of one body can then be described as being a fraction of the velocity of the other, e.g., $v_3 = \eta^{23} v_2$ ($0 \leq \eta^{23} \leq 1$) before the collision effect takes place. Here η^{23} is assumed to depend on the elasticity, or coefficient of restitution, as $\eta^{23} = 1 - \epsilon^{23}$. In

general, this leads to the following instantaneous representation at a contact point, i,

$$v_2^i = \eta^i v_1^i \tag{19}$$

with $\eta^i = 1 - \epsilon^i$ and v_1^i and v_2^i such that $v_2^i > v_1^i$.

To design a uniformly converging collision rule, the second collision in the sequence (i.e., the one between m_2 and m_3 in Fig. 1) has to take the change of velocities during the preceding, interacting, collision into account. Including this interaction in an idealized collision rule is difficult because the collisions are active only at one moment in time and partial interaction is hard to model. For Poisson's collision rule, limited interaction is possible by allowing interaction between compression and expansions phases, but this is insufficient to handle the illustrated complex interaction.

To design a more flexible collision rule, an additional phase in the collision process is introduced that accounts for the change in relative velocity as given in Eq. (19). This constraint becomes active whenever there is a *dependent* contact point where a collision takes place that affects the velocity, i.e., for a contact point i, such that $g^i = v_2^i - v_1^i$,

$$g^i = 0 \wedge \dot{g}_E^i < 0 \wedge (v_{1,E}^i \neq v_{1,A}^i \vee v_{2,E}^i \neq v_{2,A}^i). \tag{20}$$

Here the constraints on relative position and velocity determine that a collision occurs and the constraints on the individual velocities that dependent collisions are active that affect the velocities.[2]

To allow collisions to occur at nonzero velocity, the constraint in Eq. (19) has to be extended. For this case, $|v_{2,E} - v_{2,A}| > |v_{3,E} - v_{3,A}|$, and v_3 reaches a fraction of v_2 while taking an offset $v_{3,A}$ into account,

$$v_{3,E} = (1 - \epsilon^{23}) * (v_{2,E} - v_{3,A}) + v_{3,A} \tag{21}$$

or, in general, for a contact point i,

$$v_{2,E}^i = (1 - \epsilon^i) * (v_{1,E}^i - v_{2,A}^i) + v_{2,A}^i \tag{22}$$

However, in this formulation, for $\epsilon^i = 1$, $v_{2,E}^i = v_{2,A}^i$, and, therefore, $v_{2,E}^i$ is fixed. So, other simultaneous collisions cannot affect $v_{2,E}^i$, an anomalous situation. Instead, the formulation should be such that for this value of ϵ^i the velocity $v_{2,E}^i$ is not affected by the dependent collision, i.e., there is no force acting. This requires a formulation at the force (impulse) level, instead of in terms of velocities. Accounting for the substitute mass, $m_s^i = \frac{m_1^i m_2^i}{m_1^i + m_2^i}$, where m_1^i and m_2^i are the two masses involved in the collision at contact i, this leads to the formula

$$\epsilon^i \Lambda^i + (1 - \epsilon^i) m_s^i \dot{g}_E^i = 0, \quad 0 \leq \epsilon_i \leq 1 \tag{23}$$

[2]During continuous behavior, $v_{1,E}^i = v_{1,A}^i$ and $v_{2,E}^i = v_{2,A}^i$, as the left and right limit values of a point on a continuous, C^0, curve have to be equal.

Thus, for $\epsilon^i = 0$ the velocities become equal and for $\epsilon^i = 1$ there is no interaction because $\Lambda^i = 0$.

For one contact point between two masses the impulsive force acting on m_2 can be derived from Eq. (23) by writing

$$\epsilon^i m_2^i (v_{2,E}^i - v_{2,A}^i) + (1 - \epsilon^i) m_s^i (v_{2,E}^i - v_{1,E}^i) = 0 \tag{24}$$

From this, in case $m_1^i = m_2^i = 1$, Eq. (22) follows.

Putting the pieces together, the collision rule extends the standard Newton's collision rule as follows. If $g^i = 0 \wedge \dot{g}_E^i < 0$ contact behavior is evaluated based on two cases:

1. A pre-collison phase because of dependency between collisions (i.e., $v_{2,E}^i \neq v_{2,A}^i \vee v_{1,E}^i \neq v_{1,A}^i$). Behavior is computed based on an initial velocity change and by balancing forces, i.e.,
$$\begin{cases} \epsilon^i \Lambda^i + (1 - \epsilon^i) m_s^i \dot{g}_E^i = 0 \\ F_1^i = -\Lambda^i \\ F_2^i = \Lambda^i \end{cases} \tag{25}$$
with m_s^i the substitute mass.

2. Execution of the collision effect, computed based on Newton's collision rule and by balancing forces, i.e.,
$$\begin{cases} v_{2,E}^i - v_{1,E}^i = -\epsilon^i * (v_{2,A}^i - v_{1,A}^i) \\ F_1^i = -F_2^i \end{cases} . \tag{26}$$

So, behavior at the contact points is then governed by either the velocity restitution based on Newton's collision rule or by the pre-collision effect (in addition to conservation of momentum, not explicitly mentioned in the proceedings anymore). The particular contact points are elements of the sets I_k^N and I_k^P, respectively. Furthermore, the pre-collision effect is always first completed by executing Newton's collision rule after the pre-collision at that contact point, provided $\dot{g}_E^i < 0$ still holds, before new independent collisions are inferred. The forces are summed in case multiple contact points exert a force on the same mass.

In summary, the independent collision set that may trigger a sequence of collision and pre-collision effects can be specified by

$$I_k^{N_1} = \{i \in I_G | (g^i = 0 \wedge \dot{g}_E^i \leq 0) \wedge (v_{2,E}^i = v_{2,A}^i \wedge v_{1,E}^i = v_{1,A}^i)\} \tag{27}$$

and applies Newton's collision rule.[3] Because of the second clause, the sequence of pre-collision and collision effects is first completed before a possible new collision sequence is triggered.[4]

[3] Note that g^i is not indexed by either E or A as it is a C^0 variable.

[4] Alternatively, to achieve the same effect, the clause can be replaced by $I_{k-1}^P = \emptyset$.

Each pre-collision in a set I_{k-1}^P may be followed by Newton's collision rule as well, gathered in the set $I_k^{N_2}$

$$I_k^{N_2} = \{i \in I_G | i \in I_{k-1}^P \wedge (g^i = 0 \wedge \dot{g}_E^i \leq 0)\} \tag{28}$$

and $I_k^N = I_k^{N_1} \cup I_k^{N_2}$. Given these sets of contact points, $I_k^{N_1}$ and $I_k^{N_2}$, the 'intermediate' velocities $\dot{g}_P^i$ are computed using Eq. (26) with $v_{j,E}^i$ substituted for the input $v_{j,A}^i$. These are intermediate velocities as their values may cause pre-collision effects, I_k^P

$$I_k^P = \{i \in I_G | \dot{g}_P^i \leq 0\} \tag{29}$$

When all sets, $I_k^{N_1}$, $I_k^{N_2}$, and I_k^P, are determined, the velocities are updated, i.e., $v_{j,A}^i = v_{j,E}^i$, and the new $v_{j,E}^i$ are computed using Eq. (25) and Eq. (26) for the contact points in I_k^P and I_k^N, respectively.

During this sequence of computations, $v_{j,E}^i \neq v_{j,A}^i$, and, therefore, $I_{k+l}^{N_1} = \emptyset$. When the sequence of pre-collisions and collisions has terminated, $I_{k+m}^{N_2} = \emptyset$ and $\dot{g}_P^i = \dot{g}^i$, and, consequently, $I_{k+m}^P = \emptyset$ as well, where $0 < l < m$. Therefore, $v_{j,E}^i = v_{j,A}^i$ and $I_{k+m}^{N_1}$ may be populated again and further collisions may occur. The first collision is indexed $k = 1$, $I_0^P = I_0^{N_1} = I_0^{N_2} = \emptyset$, and k is reset to 0 when no further collisions occur (either dependent or independent).

The results of this new collision rule for three colliding bodies, as shown in Fig. 1, can now be compared against those for Newton and Poisson collision rules presented in Section 2. Both the Newton and Poisson collision rules did not properly transfer momentum from m_1 to m_3 in case $\epsilon^{12} = \epsilon^{23} = 1$, as can be seen in Fig. 3(a) and Fig. 4(a). The new collision rule does properly exhibit this behavior as illustrated by Fig. 6(a). In addition, Fig. 3(c) and Fig. 4(c) show the Newton and Poission collision rules to have no ϵ^{23} dependence when $\epsilon^{12} = 1$. In Fig. 6(c) the ϵ^{23} dependence of the new collision rule is shown to achieve correct values for the limit values, $\epsilon^{23} = 0$ and $\epsilon^{23} = 1$.

In case a large mass m_3 is used, mimicking a collision between two bodies, one of which is at rest on a floor (see Fig. 2), Newton's collision rule would not properly compute m_2 leaving the floor as shown in Fig. 3(b). The new collision rule does yield this behavior as shown in Fig. 6(b) and it does not produce an abrupt change in behavior for varying ϵ^{12} as illustrated for Poisson's collision rule in Fig. 4(b).

Note that for large m_3 and $\epsilon^{12} = \epsilon^{23} = 1$, similar to Poisson's collision rule, the new collision rule computes velocities that differ from the first order approximation in Table 1, entry $m_3 = 1000$, $R^{12} = 0.05$, $R^{23} = 0.05$. This approximation, however, is a crude one and real-life experiments should be performed to establish realistic behavior. Intuitively, for $\epsilon^{12} = \epsilon^{23} = 1$ a sequence of isolated collisions would occur, transfering momentum completely from m_1 to m_2, which then collides with the large mass m_3, causing m_2 to reverse its velocity

and to then transfer its momentum completely back to m_1. Therefore, m_2 would remain at rest.

4 Increasing Complexity

Because three bodies only allow two collisions, and, therefore, only analysis of one pair of dependent collisions, generality is limited. To investigate a more general situation, sequences of collisions of four bodies, as shown in Fig. 7, are analyzed. The results for varying ϵ^i are presented in Fig. 8 for $m_1 = m_2 = m_3 = m_4 = m$. Collision behavior for the different sets of active rules is derived and computed by MATLAB (MATLAB 1997) and its Symbolic Math Toolbox (SymbolicMath 2003).[5] Note that, again, collision behavior is smooth and converges between the two limit values that can be verified to match collision behavior of more detailed models.

To illustrate the execution of the collision law, consider the case where $\epsilon^{23} = 0.5$ in Fig. 8(b). The sequence of collision effects for this parameter value is given in Table 2. The velocities achieved during the collision are

$$\begin{bmatrix} {}^{k}v_1 \\ v_2 \\ v_3 \\ v_4 \end{bmatrix} = \begin{bmatrix} {}^{0}v_0 \\ 0 \\ 0 \\ 0 \end{bmatrix}, \left(\begin{bmatrix} {}^{1}0 \\ v_0 \\ 0 \\ 0 \end{bmatrix} \right), \begin{bmatrix} {}^{1}-\frac{1}{7}v_0 \\ \frac{6}{7}v_0 \\ \frac{2}{7}v_0 \\ 0 \end{bmatrix}, \left(\begin{bmatrix} {}^{2}-\frac{1}{7}v_0 \\ \frac{3}{7}v_0 \\ \frac{5}{7}v_0 \\ 0 \end{bmatrix} \right), \begin{bmatrix} {}^{2}-\frac{1}{7}v_0 \\ \frac{3}{7}v_0 \\ \frac{5}{7}v_0 \\ 0 \end{bmatrix}, \left(\begin{bmatrix} {}^{3}-\frac{1}{7}v_0 \\ \frac{3}{7}v_0 \\ 0 \\ \frac{5}{7}v_0 \end{bmatrix} \right), \begin{bmatrix} {}^{3}-\frac{1}{7}v_0 \\ \frac{15}{49}v_0 \\ \frac{3}{49}v_0 \\ \frac{38}{49}v_0 \end{bmatrix}, \begin{bmatrix} {}^{4}-\frac{1}{7}v_0 \\ \frac{6}{49}v_0 \\ \frac{12}{49}v_0 \\ \frac{38}{49}v_0 \end{bmatrix} \tag{30}$$

where the values in parentheses are the results after computing $\dot{g}_P^i$ and these are replaced because analysis shows that further (pre-)collision effects occur. Note that pre-collision effects do not trigger further pre-collision effects, otherwise, at step 1, contact 34 would be included as a pre-collision because $v_3 > v_4$.

A detailed physical explanation for this is difficult to provide as the propagation of the collision shockwaves is a complicated and still not a well-understood phenomenon. Given the accuracy of the presented model, it appears as though there is a degree of coupling between the 'secondary' contact points (those that partake in the pre-collision) that allow shockwaves of the primary collision to travel across them, the degree of which is related to the coefficient of restitution. Given this, the secondary contact points represent a first order effect, and these higher order effects of this coupling can be abstracted away from the collision model.

This observation is supported by experiments reported in (Ceanga & Hurmuzlu 2001) where an 'Impulse Transmission Ratio' is introduced similar to the coupling coefficient η in Section 3. The Impulse Transmission Ratio is applied to triplets of adjacent bodies, or two adjacent contact points, as well. Note that, in general, η can be chosen an independent parameter as opposed to substituting $\eta = 1 - \epsilon$.

[5] The MATLAB code of the collision models is available upon request.

This system also includes behavior where a pre-collision is triggered for a contact but not followed by Newton's collision rule, i.e., it does not appear in $I_1^{N_2}$. If $\epsilon^{23} = 0$, the first collision is, $I_1^{N_1} = \{1\}$, $I_1^{N_2} = \{\}$, and $I_1^P = \{2\}$ and the post velocities $v_1 = -\frac{1}{3}v_0$, $v_2 = v_3 = \frac{2}{3}v_0$, and $v_4 = 0$. The next iteration yields $I_1^{N_1} = \{\}$, $I_1^{N_2} = \{\}$, and $I_1^P = \{\}$ because $v_{j,E}^i \neq v_{j,A}^i,\ i \in \{1,2,3\},\ j \in \{1,2\}$, and, therefore, contact 34 is not included in $I_1^{N_1}$. After the $v_{j,A}^i$ are updated, the collision computation is resumed with $I_2^{N_1} = \{3\}$, $I_2^{N_2} = \{\}$, and $I_2^P = \{2\}$.

The presented extended collision rule is still sensitive to initial value perturbations. Consider the mass distribution $m_1 = 1$, $m_2 = 0.1$, $m_2 = 1$, and $m_3 = 1$. For $0 \leq \epsilon^{23} \leq 1$ the velocities after collision are shown in Fig. 9. For certain values of ϵ^{23}, discontinuous changes in final velocities occur. This is caused by a change in the sequence of active contact points when it includes simultaneous collisions, i.e., $I_k^{N_2}$ has size larger than 1, see the results in Table 3. Even when such a collision is triggered with very small relative velocity, it causes a significant change in the post collision velocities. This may be prevented by invoking a pre-collision stage as well when collisions with low relative velocity take place. The effect of these pre-collisions can gradually decrease until for larger relative velocity a true collision takes place, i.e., $\eta^i = f(\dot{g}^i)$. Future work will concentrate on further exploring this.

5 Conclusions

Often, in collision models the normal component is handled by either a Newton or Poisson type collision law. In case of multiple impacts, the collisions are assumed to occur at the same point in time and to be synchronized in terms of their compression and expansion behavior.

This assumption is violated when sequences of dependent collisions occur and compression and expansion phases overlap. In the limit cases, i.e., restitution coefficients of value 0 and 1, either all constraints need to be activated simultaneously or sequentially. This is discussed in detail in other work (Mosterman & Breedveld 1999). Because of the two different methods of handling the limit cases, there is no uniform convergence between them based on one type of activation constraint only.

This paper presents a method where a pre-collision phase precedes the application of Newton's collision rule in case of multiple dependent sequential collisions. It is shown how the resulting characteristic converges uniformly between the limit cases. Furthermore, it is shown that this extended collision rule conforms better with a linear first order approximation.

Because of the superior characteristics of Poisson's collision rule for multiple contacts (Pfeiffer & Glocker 1996), future work concentrates on extending this collision rule similarly. Furthermore, sensitivity to simultaneous independent collisions is further investigated.

6 Acknowledgement

During this work, Pieter J. Mosterman was supported by a grant from the DFG Schwerpunktprogramm KONDISK and employed by the German Aerospace Center (DLR) Oberpfaffenhofen. Mehmet Yunt provided some valuable comments on an earlier draft of this paper that are much appreciated.

References

Brach, R. M. 1991. *Mechanical Impact Dynamics.* New York: John Wiley and Sons.

Brogliato, B. 1999. *Nonsmooth Mechanics.* London: Springer-Verlag. ISBN 1-85233-143-7.

Ceanga, V., and Hurmuzlu, Y. 2001. A new look at an old problem: Newton's cradle. *Journal of Applied Mechanics* 68(4):575–583.

Chatterjee, A., and Ruina, A. 1998. A new algebraic rigid body collision law based on impulse space considerations. *Journal of Applied Mechanics.*

Chatterjee, A. 1999. On the realism of complementarity conditions in rigid body collisions. *Nonlinear Dynamics* 20:159–168.

Glocker, C. 1995. *Dynamik von Starrkörpersystemen mit Reibung und Stößen.* PhD dissertation, Technical University of Munich, Germany. in German.

Ivanov, A. P. 1995. On multiple impact. *Journal of Applied Mathematics and Mechanics* 59(6):887–902.

Lötstedt, P. 1981. Coulomb friction in two-dimensional rigid body systems. *Z. angew. Math. u. Mech.* 61:605–615.

MATLAB. 1997. *The Language of Technical Computing.* The MathWorks.

Mosterman, P. J., and Biswas, G. 1999. A Java Implementation of an Environment for Hybrid Modeling and Simulation of Physical Systems. In *ICBGM99*, 157–162.

Mosterman, P. J., and Breedveld, P. 1999. Some Guidelines for Stiff Model Implementation with the Use of Discontinuities. In *ICBGM99*, 175–180.

Mosterman, P. J. 2002. HYBRSIM – a modeling and simulation environment for hybrid bond graphs. *Journal of Systems and Control Engineering* 216:35–46. special issue paper.

Pfeiffer, F., and Glocker, C. 1996. *Multibody dynamics with unilateral contacts.* New York: John Wiley & Sons, Inc.

SymbolicMath. 2003. *Symbolic Math Toolbox User's Guide.* The MathWorks, Natick, MA.

List of Figures

1 A sequence of dependent collisions. 15
2 Collision between two bodies and a floor. 15
3 Resulting velocities for Newton's collision rule. 16
4 Resulting velocities for Poisson's collision rule. 16
5 Different elasticity leads to differences in relative velocity. 16
6 Resulting velocities for the new collision rule. 17
7 A sequence of four colliding bodies. 17
8 Resulting velocities for the new collision rule. 17
9 Final velocities for $m_2 = 0.1$ and $0 \leq \epsilon^{23} \leq 1$. 17

List of Tables

1 Benchmark results of numerical linear approximation. 15
2 Collision sets. 15
3 Collision sets, $m_2 = 0.1$, $\epsilon^{23} = 0.6$. 15

Table 1: Benchmark results of numerical linear approximation.

$C^{12}=0.1$, $C^{23}=0.1$, $m_1=1.0$, $m_2=1.0$					
m_3	R^{12}	R^{23}	v_1	v_2	v_3
1000	0.05	0.05	-0.9744439	-0.21306606	0.0021875096
1000	50	0.05	-0.48997312	-0.4817458	0.0019684185
1000	0.05	50	-0.9101933	-0.00493735	0.00191513
1.0	0.05	0.05	-0.13018857	0.15019388	0.9799948
1.0	50	0.05	0.16781114	0.17072338	0.6614654
1.0	0.05	50	-0.32068235	0.65912620	0.6615559

Table 2: Collision sets.

k	$I_k^{N_1}$	$I_k^{N_2}$	I_k^P
1	$\{1\}$	$\{\}$	$\{2\}$
2	$\{\}$	$\{2\}$	$\{3\}$
3	$\{\}$	$\{3\}$	$\{2\}$
4	$\{\}$	$\{2\}$	$\{\}$

Table 3: Collision sets, $m_2=0.1$, $\epsilon^{23}=0.6$.

k	$I_k^{N_1}$	$I_k^{N_2}$	I_k^P
1	$\{1\}$	$\{\}$	$\{2\}$
2	$\{\}$	$\{2\}$	$\{1,3\}$
3	$\{\}$	$\{1,3\}$	$\{2\}$
4	$\{\}$	$\{2\}$	$\{1\}$
5	$\{\}$	$\{1\}$	$\{2\}$
6	$\{\}$	$\{2\}$	$\{1,3\}$
7	$\{\}$	$\{1,3\}$	$\{\}$

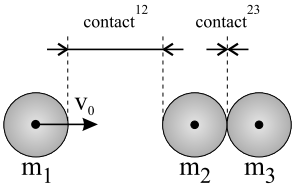

Figure 1: A sequence of dependent collisions.

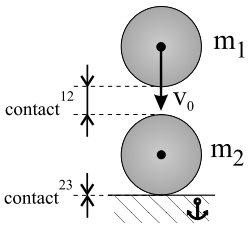

Figure 2: Collision between two bodies and a floor.

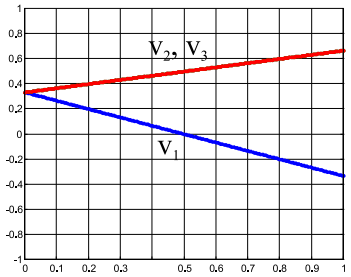

(a) As a function of ϵ^{12}.

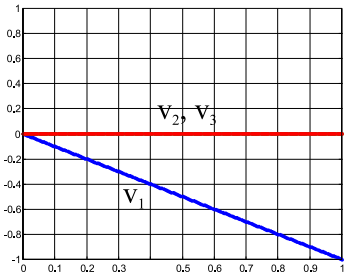

(b) As a function of ϵ^{12} with m_3 large.

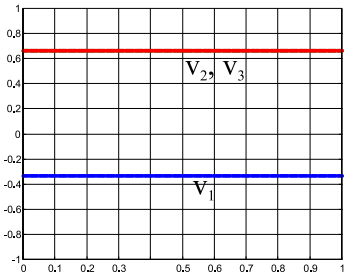

(c) As a function of ϵ^{23}.

Figure 3: Resulting velocities for Newton's collision rule.

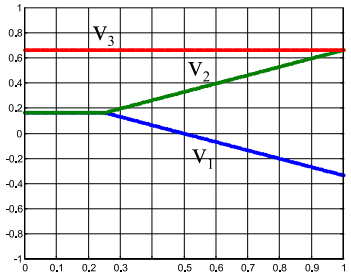

(a) As a function of ϵ^{12}.

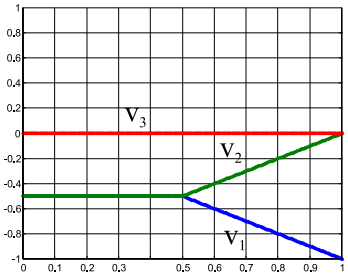

(b) As a function of ϵ^{12} with m_3 large.

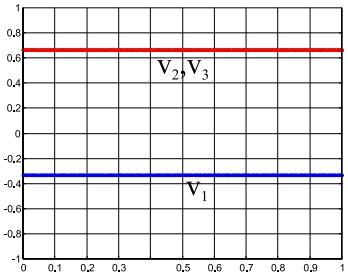

(c) As a function of ϵ^{23}.

Figure 4: Resulting velocities for Poisson's collision rule.

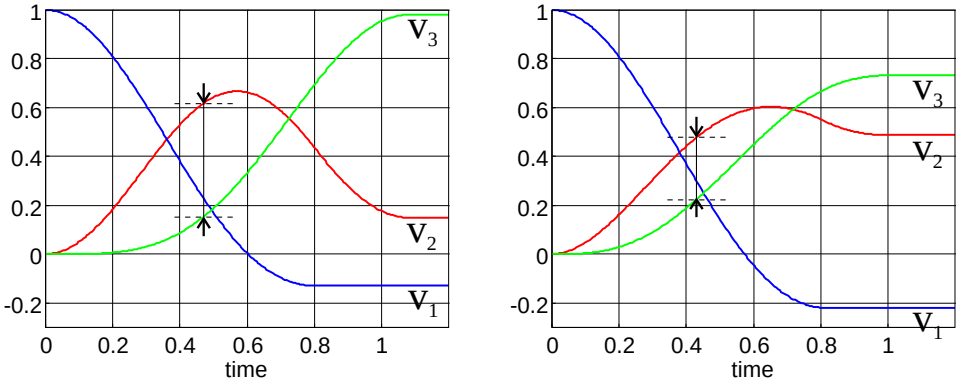

Figure 5: Different elasticity leads to differences in relative velocity.

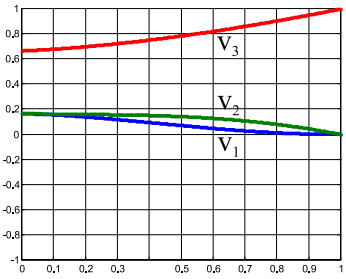

(a) As a function of ϵ^{12}.

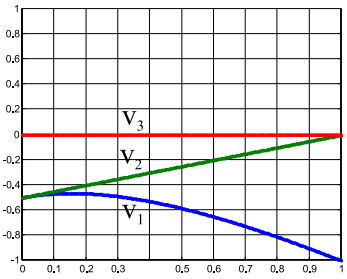

(b) As a function of ϵ^{12} with m_3 large.

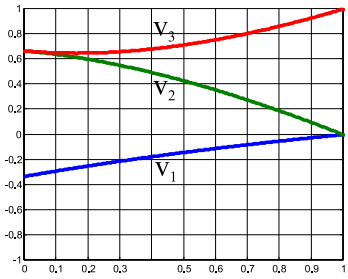

(c) As a function of ϵ^{23}.

Figure 6: Resulting velocities for the new collision rule.

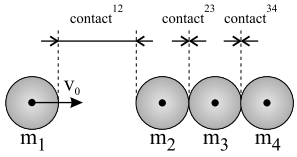

Figure 7: A sequence of four colliding bodies.

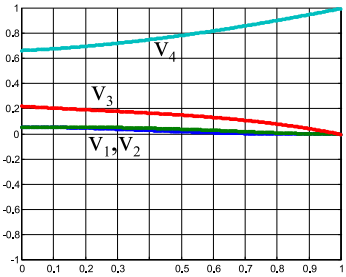

(a) As a function of ϵ^{12}.

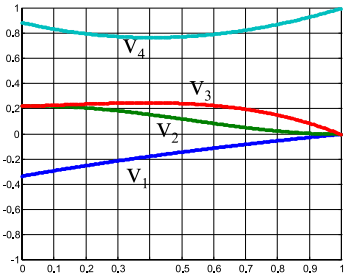

(b) As a function of ϵ^{23}.

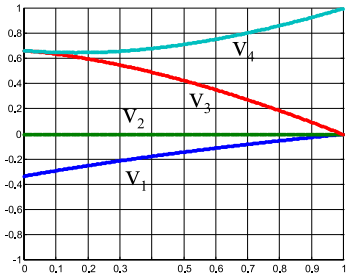

(c) As a function of ϵ^{34}.

Figure 8: Resulting velocities for the new collision rule.

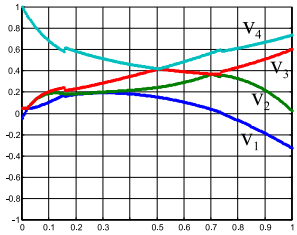

Figure 9: Final velocities for $m_2 = 0.1$ and $0 \leq \epsilon^{23} \leq 1$.